Transp Porous Med (2012) 93:63–77
DOI 10.1007/s11242-012-9944-9

# Generalized Solution for 1-D Non-Newtonian Flow in a Porous Domain due to an Instantaneous Mass Injection

**Vittorio Di Federico · Valentina Ciriello**

Received: 2 August 2011 / Accepted: 16 January 2012 / Published online: 31 January 2012


**Abstract** Non-Newtonian fluid flow through porous media is of considerable interest in several fields, ranging from environmental sciences to chemical and petroleum engineering. In this article, we consider an infinite porous domain of uniform permeability $k$ and porosity $\phi$, saturated by a weakly compressible non-Newtonian fluid, and analyze the dynamics of the pressure variation generated within the domain by an instantaneous mass injection in its origin. The pressure is taken initially to be constant in the porous domain. The fluid is described by a rheological power-law model of given consistency index $H$ and flow behavior index $n$; $n, < 1$ describes shear-thinning behavior, $n > 1$ shear-thickening behavior; for $n = 1$, the Newtonian case is recovered. The law of motion for the fluid is a modified Darcy's law based on the effective viscosity $\mu_{ef}$, in turn a function of $\phi$, $H$, $n$. Coupling the flow law with the mass balance equation yields the nonlinear partial differential equation governing the pressure field; an analytical solution is then derived as a function of a self-similar variable $\eta = rt^{\beta}$ (the exponent $\beta$ being a suitable function of $n$), combining spatial coordinate $r$ and time $t$. We revisit and expand the work in previous papers by providing a dimensionless general formulation and solution to the problem depending on a geometrical parameter $d$, valid for plane ($d = 1$), cylindrical ($d = 2$), and semi-spherical ($d = 3$) geometry. When a shear-thinning fluid is considered, the analytical solution exhibits traveling wave characteristics, in variance with Newtonian fluids; the front velocity is proportional to $t^{(n-2)/2}$ in plane geometry, $t^{(2n-3)/(3-n)}$ in cylindrical geometry, and $t^{(3n-4)/[2(2-n)]}$ in semi-spherical geometry. To reflect the uncertainty inherent in the value of the problem parameters, we consider selected properties of fluid and matrix as independent random variables with an associated probability distribution. The influence of the uncertain parameters on the front position and the pressure field is investigated via a global sensitivity analysis evaluating the associated Sobol' indices. The analysis reveals that compressibility coefficient and flow behavior index are the most

V. Di Federico (✉) · V. Ciriello
Dipartimento di Ingegneria Civile, Ambientale e dei Materiali (DICAM),
Università di Bologna, Bologna, Italy
e-mail: vittorio.difederico@unibo.it

V. Ciriello
e-mail: valentina.ciriello3@unibo.it

influential variables affecting the front position; when the excess pressure is considered, compressibility and permeability coefficients contribute most to the total response variance. For both output variables the influence of the uncertainty in the porosity is decidedly lower.

**Keywords** Non-Newtonian · Porous medium · Self-similar solution · Sobol' indices · Polynomial chaos expansion

## 1 Introduction

Non-Newtonian fluid flow through porous media is of considerable interest in petroleum and environmental engineering.

In reservoir engineering, heavy and waxy oils often display significant non-Newtonian behavior. Several fluids used to enhance oil recovery from underground reservoirs exhibit shear-dependence of viscosity and other distinctly non-linear effects. During water flooding operations, chemical additives, polymeric solutions or foams are routinely added to the injected water to improve the overall sweeping efficiency and minimize the instability effects; surfactants are also added to the water phase to decrease the surface tension between the aqueous and oil phases. Fracturing agents and drilling muds with complex rheologic behavior are also commonly used in low-permeability formations.

In environmental applications, liquid pollutants and wastes may migrate in the subsurface and penetrate underground reservoirs, leading to groundwater contamination; several of those, such as suspensions, solutions and emulsions of various substances, certain asphalts and bitumen, greases, sludges, and slurries, are distinctly non-Newtonian. Non-linear fluid flow in porous media may also be relevant in soil remediation processes involving the removal of liquid pollutants via chemical (often polymerization) reactions.

The scientific and engineering relevance of the aforementioned applications has generated a large body of literature, aimed at an understanding of non-Newtonian fluid flow in porous media. For exhaustive reviews on this topic, see Savins (1969), Goldstein and Entov (1994), Shenoy (1995), as well as the more recent one by Chhabra et al. (2001), mainly geared toward man-made porous media.

Available approaches to describe non-Newtonian flow in porous media may be broadly classified as pore-scale network models and continuum models (Sochi 2010).

In the first case, the space between pores is modeled as a network of channels with idealized geometry. Relations describing the transport properties at the channel scale are upscaled to compute effective properties at a larger scale. Pore-scale models, while fully incorporating basic laws, rely on an idealized representation of the porous medium geometry.

Continuum models, on the other hand, incorporate a closed-form, relatively simple constitutive equation at the Darcy scale describing the relation between pressure gradient and specific flux; this relation is often a modification of Darcy's law. Ignoring the physics of flow at pore level, continuum models have been criticized as unable to represent time-dependent effects and to model flow of yield-stress fluids.

Different formulations of the modified Darcy law for non-Newtonian fluids have been proposed (Bird et al. 1960; Christopher and Middleman 1965; Kozicki 1967; Teeuw and Hesselink 1980; Pearson and Tardy 2002), particularly for pseudoplastic fluids described by a power-law model. Many of these models have been derived using a capillary representation of the porous medium, and include a constant related to its tortuosity.

In turn, these formulations have been used for large-scale reservoir modeling, in conjunction with the continuity equation. While in complex geometries a solution of the flow problem

often requires a numerical approach (Wu and Pruess 1998), analytical solutions in simple geometries readily allow sensitivity analysis. In the 1980s and 1990s, Pascal and coworkers studied, in a series of papers (see Pascal and Pascal 1997 for a partial list of references), flow within natural porous media saturated by non-Newtonian fluids described by a power-law rheology; consequently, the applicable flow law is a modified nonlinear Darcy's law. In all these papers, the nonlinear flow problem is solved via the adoption of a self-similar variable, widely employed in engineering mathematics (Barenblatt 1996). The adoption of a self-similar solution allows derivation of closed-form solutions for transient problems, albeit with limitations on the type of initial and boundary conditions allowed.

In this article, we revisit and expand previous work by Pascal (1991a,b) on the dynamics of the pressure variation generated within an infinite porous domain, initially at uniform pressure and saturated by a weakly compressible non-Newtonian fluid, by an instantaneous mass injection in the origin. We do so by providing a dimensionless formulation of the problem depending on a geometrical parameter $d$, valid for plane ($d = 1$), cylindrical ($d = 2$), and semi-spherical ($d = 3$) geometry; we then derive a self-similar solution to the problem which generalizes previous results. The closed-form solution thus obtained is a function of the problem parameters, regrouped into dimensionless groups; some of the former, most notably the fluid flow behavior index, and the domain properties (permeability, porosity, and porous medium compressibility coefficient) are amenable to uncertainty; in turn, this renders uncertain the output variables, i.e., the pressure front position and velocity and the pressure distribution within the domain. To analyze the sensitivity of the output variables to parameter uncertainty, we conduct a global sensitivity analysis (GSA) with the computation of Sobol' indices; the latter are evaluated by means of the polynomial chaos expansion (PCE) technique, introduced in the engineering field by Ghanem and Spanos (1991) in the context of the stochastic finite elements analysis.

## 2 Problem Formulation

We consider an infinite porous domain, initially saturated by a weakly compressible non-Newtonian fluid, and analyze the dynamics of the pressure variation generated within the domain by an instantaneous mass injection.

The pressure is taken to be uniform in the porous domain at time $t = 0$, when a given fluid mass $m_0$ is instantaneously injected at a well located in the domain origin (Fig. 1); we

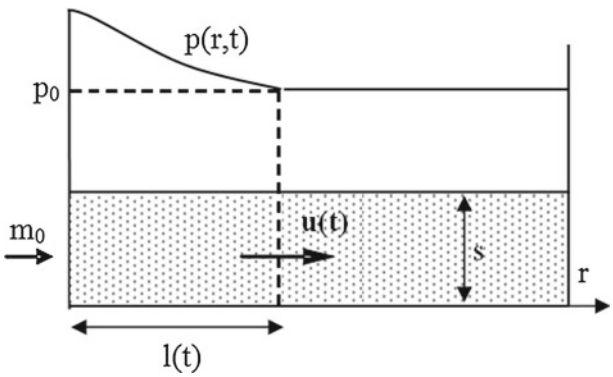


**Fig. 1** Domain schematic

consider plane ($d = 1$), cylindrical ($d = 2$), and semi-spherical ($d = 3$) geometry. Hence, the domain thickness is $s$ for $d = 1, 2$, while the well radius is zero for $d = 1$, and $r_w$ for $d = 2, 3$; correspondingly, the injection face is $\delta s^2$ for $d = 1$ ($\delta$ being the ratio between the transversal and the vertical dimension of the area perpendicular to flow), $2\pi s r_\mathrm{w}$ for $d = 2$, and $2\pi r_\mathrm{w}^2$ for $d = 3$.

The fluid is described by the rheological power-law model, given for simple shear flow by

$$\tau = H\dot{\gamma}\,|\dot{\gamma}|^{n-1}\,, \tag{1}$$

in which $\tau$ is the shear stress, $\dot{\gamma}$ is the shear rate, $H$ is the fluid consistency index, and $n$ is the flow behavior index (a positive real number). When $n < 1$, the model describes pseudoplastic behavior, whereas $n > 1$ represents dilatant behavior; $n = 1$ means Newtonian fluid; in the latter case, $H$ reduces to Newtonian viscosity $\mu$.

The flow law for the fluid is a modified Darcy's law taking into account the nonlinearity of the rheological equation, proposed by Bird et al. (1960) and later adopted by other authors (Savins 1969; Shenoy 1995; Di Federico et al. 2010). Thus, the flow and continuity equation for injection ($\partial p/\partial r < 0$) are, respectively:

$$v = \left(-\frac{k}{\mu_\mathrm{ef}}\frac{\partial p}{\partial r}\right)^{1/n}, \tag{2}$$

$$\frac{\partial v}{\partial r} + \frac{(d-1)\,v}{r} = -\left(\phi \cdot c_0 + c_p\right)\frac{\partial p}{\partial t}, \tag{3}$$

where $r$ is the spatial coordinate, $t$ is the time, $v$ is the Darcy velocity, $p$ is the pressure, $c_0$ is the fluid compressibility coefficient, $c_\mathrm{p}$ is the porous medium compressibility coefficient, $\phi$ is the porosity, $k$ is the permeability coefficient, $\mu_\mathrm{ef}$ is the effective viscosity; in turn, the latter is a function of $\phi$, $H$, $n$, according to (Pascal and Pascal 1985)

$$\frac{k}{\mu_\mathrm{ef}} = \frac{1}{2H}\left(\frac{n\phi}{3+n}\right)^n \left(\frac{8k}{\phi}\right)^{(1+n)/2}. \tag{4}$$

Substituting Eq. 2 in Eq. 3, one obtains:

$$\frac{\partial^2 p}{\partial r^2} + \frac{(d-1)\,n}{r}\frac{\partial p}{\partial r} = n\left(\phi \cdot c_0 + c_p\right)\left(\frac{\mu_\mathrm{ef}}{k}\right)^{1/n}\left(\frac{\partial p}{\partial r}\right)^{(n-1)/n}\frac{\partial p}{\partial t}. \tag{5}$$

The initial condition throughout the domain is

$$p(r, t = 0) = p_0, \tag{6}$$

while the mass conservation law requires that the fluid mass $m_0$ released into the domain at $t = 0$ is conserved:

$$m_0 = \omega s^{3-d}\rho\left(\phi \cdot c_0 + c_\mathrm{p}\right)\int_0^{l(t)} (p - p_0)\cdot r^{d-1}\mathrm{d}r, \tag{7}$$

where $\rho$ is fluid density. In (7), the well radius $r_\mathrm{w}$ is taken to be zero for $d = 2, 3$; the factor $\omega$ takes the value $\delta$ for $d = 1$, and the value $2\pi$ for $d = 2, 3$; $l(t)$ represents the distance at which the pressure perturbation induced by the mass injection propagates within the porous domain. For first-type boundary conditions at the origin in lieu of (7), Pascal and Pascal (1985) showed that for $n < 1$, a pressure front propagates from the origin into the domain with finite velocity; the pressure front separates the portion of the domain affected by pumping/injection from that left still undisturbed; at and beyond the compression front,

the Darcy velocity is null and the fluid remains at the constant pressure $p_0$; thus, at any given time $t < \infty$, $l(t)$ is finite.

For $n < 1$, if $l(t)$ is the front position and $u(t) = \phi \mathrm{d}l/\mathrm{d}t$ is its velocity, one has

$$p[l(t), t] = p_0, \tag{8}$$

$$\left(\frac{\partial p}{\partial r}\right)_{r=l(t)} = 0, \tag{9}$$

$$l(t=0) = 0. \tag{10}$$

For $n \geq 1$, no pressure front exists, and $l(t) \to \infty$ for any $t$; hence one would need to consider the boundary condition $\lim_{r\to\infty} p(r) = p_0$ in lieu of Eqs. 8–10.

In the following, we consider only the case of pseudoplastic fluid flow ($n < 1$), which is undoubtedly more common in field applications (Pearson and Tardy 2002).

In the mathematical statement of the problem given by (5–10), in principle all parameters (fluid properties, injected mass, domain geometry, porous medium properties) are subject to uncertainty, and thus amenable to a statistical treatment. However, the uncertainty associated with some of them, namely the fluid flow behavior index $n$ (difficult to determine for non-Newtonian fluids), and the domain properties (permeability $k$, porosity $\phi$, and porous medium compressibility coefficient $c_\mathrm{p}$) is decidedly larger; hence in the following we will treat $n, k, \phi, c_\mathrm{p}$ as random variables with a given mean value and probability distribution, while the remaining variables will be considered as deterministic.

## 3 Dimensionless Variables

In the following, we define dimensionless variables and groups relevant to the problem at hand; our choice of dimensionless quantities takes into account the nature of random variables of the permeability $k$ and the porous medium compressibility coefficient $c_\mathrm{p}$. In terms of notation, dimensionless variables are defined via capital letters as follows:

$$\begin{aligned}&(R, S, L, T, P, P_0, V, U, M_0, K, C_\mathrm{p})\\ &= \left(\frac{r}{\hat{L}}, \frac{s}{\hat{L}}, \frac{l}{\hat{L}}, \frac{t}{\hat{T}}, \frac{p}{\hat{P}}, \frac{p_0}{\hat{P}}, \frac{v\hat{T}}{\hat{L}}, \frac{u\hat{T}}{\hat{L}}, \frac{m_0}{\rho\hat{L}^3}, \frac{k}{\langle k\rangle}, \frac{c_\mathrm{p}}{\langle c_\mathrm{p}\rangle}\right)\end{aligned} \tag{11}$$

where $\hat{L}$ is a generic length scale, $\hat{P} = 1/\langle c_\mathrm{p}\rangle$ the pressure scale, and $\hat{T}$ is a timescale, given by

$$\hat{T} = \left(H^{1/n}\hat{L}^{(n+1)/n}/\hat{P}^{1/n}\langle k\rangle^{(n+1)/2n}\right). \tag{12}$$

With $\hat{L} \approx 10$ m, $\hat{P} = 1/\langle c_\mathrm{p}\rangle \approx 10^9$ Pa, $H \approx 1$ Pa s$^\mathrm{n}$, $\langle k\rangle \approx 10^{-12}$ m$^2$, one has $\hat{T} \approx 10^3$ s for $n = 0.5$.

With the help of Eq. 4, this recasts Eqs. 2 and 5, respectively, in the following dimensionless forms:

$$V = \frac{\chi_n^{1/n}}{\phi^{(1-n)/2n}}\left(-\frac{\partial P}{\partial R}\right)^{1/n}, \tag{13}$$

$$\frac{\partial^2 P}{\partial R^2} + \frac{(d-1)\,n}{R}\frac{\partial P}{\partial R} = nA\left(-\frac{\partial P}{\partial R}\right)^{(n-1)/n}\frac{\partial P}{\partial T}, \tag{14}$$

where

$$\chi_n = \frac{8^{(1+n)/2}}{2}\left(\frac{n}{3+n}\right)^n, \tag{15}$$

$$A = (r_c\phi + C_p)\frac{\phi^{(1-n)/2n}}{\chi_n^{1/n} K^{(1-n)/2n}}, \tag{16}$$

where $r_c = c_0/\langle c_p\rangle$ is the ratio between the fluid compressibility and the mean value of the porous medium compressibility. For a Newtonian fluid equations, (15)–(16) yield $\chi_n = 1$ and $A = (r_c\phi + C_p)$, while Eq. 14 reduces to the usual porous medium equation.

Equations 6, 8–10 expressing initial and boundary conditions are formally unchanged, except that dimensionless quantities (capital letters) replace dimensional ones. The condition given by Eq. 7 becomes instead

$$M_0 = \omega S^{3-d}(r_c\phi + C_p)\int_0^{L(T)} (P - P_0)\cdot R^{d-1}\mathrm{d}R. \tag{17}$$

## 4 Solution of the Problem

We seek a self-similar solution of the form (Barenblatt 1996; Pascal 1991a,b)

$$P = P_0 + T^{-\alpha} f(\eta); \quad \eta = RT^{-\beta}. \tag{18}$$

With (18), the conditions at the pressure front (8) and (9) transform into

$$P(\eta_1) = P_0, \tag{19}$$

$$\left(\frac{\mathrm{d}P}{\mathrm{d}\eta}\right)(\eta_1) = 0, \tag{20}$$

in which the position of the moving interface is given by

$$\eta_1 = LT^{-\beta}. \tag{21}$$

Adopting (18) shows that in order to reduce (14) to an ODE in $\eta$ requires

$$\alpha\left(1 - \frac{1}{n}\right) = -1 + \beta\left(1 + \frac{1}{n}\right). \tag{22}$$

In this case, (14) yields

$$\frac{\mathrm{d}}{\mathrm{d}\eta}\left[\eta^{d-1}\left(-\frac{\mathrm{d}f}{\mathrm{d}\eta}\right)^{1/n}\right] = A\left(\alpha\eta^{d-1} f + \beta\eta^d\frac{\mathrm{d}f}{\mathrm{d}\eta}\right). \tag{23}$$

Now taking $\alpha = d\beta$ in (23) leads to

$$\alpha = \frac{dn}{n+1+d\,(1-n)}, \beta = \frac{n}{n+1+d\,(1-n)} \tag{24}$$

$$\frac{\mathrm{d}}{\mathrm{d}\eta}\left[\eta^{d-1}\left(-\frac{\mathrm{d}f}{\mathrm{d}\eta}\right)^{1/n}\right] = A\frac{\mathrm{d}}{\mathrm{d}\eta}(\beta\eta^d f). \tag{25}$$

Equation 25 is easily integrated with the boundary condition (20), yielding

$$\left(-\frac{\mathrm{d}f}{\mathrm{d}\eta}\right)^{1/n} = A\beta\eta f. \tag{26}$$

A further integration, considering (18) and (19), gives the pressure field for $\eta < \eta_1$ as

$$P(\eta, T) = P_0 + BT^{-\mathrm{d}\beta}\eta_1^{(1+n)/(1-n)}\left[1 - \left(\frac{\eta}{\eta_1}\right)^{1+n}\right]^{1/(1-n)},$$
$$B = \left[\frac{1-n}{1+n}(A\beta)^n\right]^{1/(1-n)}. \tag{27}$$

With (18), (21), (24), and (27), the boundary condition (17) transforms into

$$M_0 = \omega S^{3-d}(r_c\phi + C_p)B\eta_1^{[1+n+d(1-n)]/(1-n)}\int_0^1 \tau^{d-1}(1-\tau^{1+n})^{1/(1+n)}\mathrm{d}\tau. \tag{28}$$

Integration of (28) (Gradshteyn and Ryzhik 2000, Eq. 3.251.1, p. 322) yields the value of the self-similar variable at the pressure front as

$$\eta_1 = \left[\frac{M_0}{\omega S^{3-d}\left(r_c\phi + C_p\right)BE}\right]^{(1-n)/[1+n+d(1-n)]}, \tag{29}$$

$$E = \frac{1-n}{1+n+d(1-n)}\frac{\Gamma[d/(1+n)]\cdot\Gamma[(2-n)/(1-n)]}{\Gamma[(1+n+d(1-n))/((1+n)(1-n))]}, \tag{30}$$

in which $\Gamma(\cdot)$ is the gamma function. Once $\eta_1$ is determined via (29), the pressure field in fully known through (27). The velocity for $\eta < \eta_1$ is then given by

$$V = \frac{\chi_n^{1/n}}{\phi^{(1-n)/2n}}\left(\frac{1-n}{1+n}A\beta\right)^{1/(1-n)}T^{-[(1+d)]/[1+n+d(1-n)]}\eta\left(\eta_1^{1+n} - \eta^{1+n}\right)^{1/(1-n)}. \tag{31}$$

Finally, the front position and velocity are respectively

$$L(T) = \eta_1 T^{n/[1+n+d(1-n)]}, \quad U(T) = \frac{n\phi}{1+n+d(1-n)}\eta_1 T^{-[1+d(1-n)]/[1+n+d(1-n)]}. \tag{32}$$

## 5 Discussion of Results

In this section, we discuss the behavior of the variables of interest as functions of the dimensionless parameters describing fluid properties, geometry and injection rate. Preliminarily, we conduct a succinct literature review on the typical ranges of variation of all input parameters involved, to deduce the corresponding intervals for dimensionless quantities.

The flow behavior index $n$ is found to vary between 0.2 and 1 in laboratory and field applications (Di Federico et al. 2010 and references therein), with a significant numbers of cases in the midrange of this interval; the fluid consistency index $H$ is inversely proportional to the flow behavior index, and takes values between 0.27 and 3.24 Pa $\mathrm{s}^n$ for solutions of polymers in liquids with $n = 0.41 \div 0.96$ (Christopher and Middleman 1965, Park et al. 1975). The fluid compressibility coefficient $c_0$ lies in the range $1 \div 5 \times 10^{-9}$ $\mathrm{Pa}^{-1}$ (Pascal 1991b) in

reservoir applications; for brine compressibility in $CO_2$ storage applications, lower values in the range $3 \div 6 \times 10^{-10}$ Pa$^{-1}$, depending on depth and salinity (Thibeau and Mucha 2011), are usually considered. The aquifer compressibility coefficient $c_p$ has typically a somewhat larger interval of variation than $c_0$, varying between $10^{-9}$and $10^{-7}$ Pa$^{-1}$ in the aquitards cited by Ostendorf et al. (2010), and between $10^{-10}$and $10^{-8}$ Pa$^{-1}$ for limestones and sandstones, depending on their degree of consolidation (Thibeau and Mucha 2011). Porosity $\phi$ may vary in the range $0.10 \div 0.40$, and permeabilities span a few orders of magnitude, ranging typically between $10^{-14}$and $10^{-10}$ m$^2$. Finally, typical pressures in field applications vary between 1 and 10 MPa in $CO_2$ injection projects, and in the range 5-40 MPa in reservoir engineering.

Hence, values of the ratio $r_c = c_0/\langle c_p \rangle$ may take values ranging from 0.005 (fluid compressibility negligible with respect to porous medium compressibility) to 500 (porous medium compressibility negligible with respect to fluid compressibility); in the following, a value $r_c = 1$ will be considered. We further assume to lead our analysis for the geometrical reference case $S = 1$, and take for the sake of simplicity $\omega = \delta = 2\pi$ when $d = 1$, (plane case), in order to be able to compare results for different values of $d$, using the cylindrical geometry ($d = 2$) as the reference case.

The output variables of interest are essentially the dimensionless pressure front position $L\,(T)$ and the dimensionless pressure in the domain in excess of the initial value $\Delta P\,(\eta, T) = P\,(\eta, T) - P_0$.

A traditional sensitivity analysis, conducted considering deterministic values of model parameters in their whole range of variability (Di Federico and Ciriello 2011), revealed that the front position is a markedly increasing function of flow behavior index $n$ and is inversely dependent on $d$. The pressure front advances at a slower rate for larger values of the compressibility coefficients, for a higher injected mass and a lower porosity; the increase of the front velocity for less compressible media is compounded for smaller values of the geometrical parameter $d$. When pressure in excess of the initial value is considered, it is seen that switching from plane to radial and from radial to spherical geometry brings about an almost order of magnitude reduction. An increase in compressibility implies a significant decrease in excess pressure, especially at early times.

Here we take a different approach considering a hypothetical case study (i.e., a specific fluid and porous medium) and selected properties of fluid and matrix modeled as independent random variables. We choose uniform distributions to represent the uncertainty connected to them as specified in Table 1, where a variability of $\pm 50\%$ around the mean value was selected for the permeability; $\pm 25\%$ for the compressibility and porosity; $\pm 10\%$ for the flow behavior index.

The influence of the uncertainty parameters on the front position and the pressure field is investigated by means of a GSA with the computation of Sobol' indices (Appendix A.1). The indices are defined by means of the PCE technique (Appendix A.2) to minimize the computational cost of the analysis.

**Table 1** Intervals of variability of the selected uniformly distributed random parameters

| Random parameter | Distribution |
|---|---|
| $\phi$ | U(0.15–0.25) |
| $K$ | U(0.50–1.50) |
| $C_p$ | U(0.75–1.25) |
| $n$ | U(0.45–0.55) |

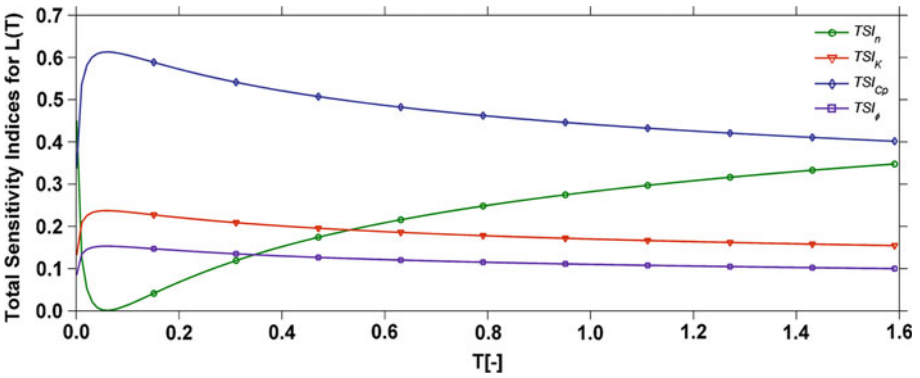


**Fig. 2** Total sensitivity indices ($TSI$) of each random parameter ($n, K, C_\mathrm{p}, \phi$) with respect to the front position $L(T)$ versus time $T$ for cylindrical geometry ($d = 2$), $S = 1$, and $r_\mathrm{c} = 1$

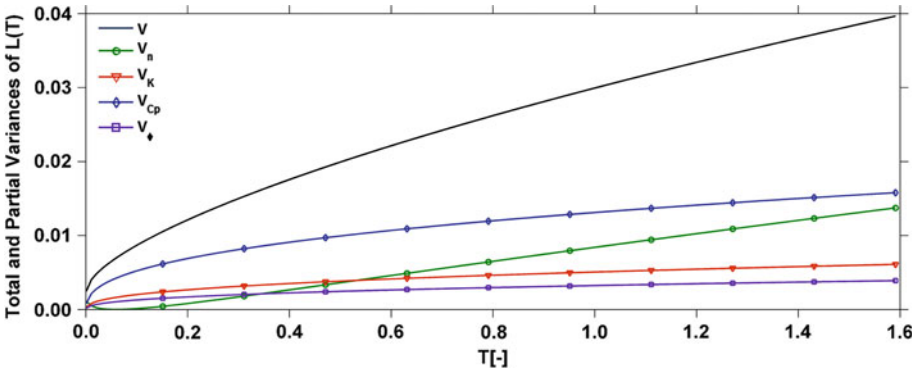


**Fig. 3** Total variance and partial variances ($V$) due to each random parameter ($n, K, C_\mathrm{p}, \phi$) with respect to the front position $L(T)$ versus time $T$ for cylindrical geometry ($d = 2$), $S = 1$, and $r_\mathrm{c} = 1$

First we observe that in all our computations the total and principal sensitivity indices were practically coincident, indicating the absence of interactions between the random parameters; for this reason the calculation of the second-order Sobol' indices yields negligible results.

Figure 2 depicts the total sensitivity indices of each random parameter with respect to the front position as a function of dimensionless time. It is seen that, with the exception of very early times, the most influential variable is the aquifer compressibility coefficient $C_\mathrm{p}$. In any case, its importance decreases in time after reaching a maximum value; the reverse is true for the flow behavior index $n$, whose total sensitivity index is high for very early times, then decreases reaching a minimum, then increases almost linearly with time for $T > 1$. As far as the porosity and the permeability are concerned, the trend of the respective total sensitivity indices is very similar, and its value is always between 10 and 25%. Figure 3 illustrates the corresponding behavior of the variances as a function of time. We find that the total variance increases, as expected, with time; the larger contribution to the total variance is due to compressibility, next to flow behavior index, then to permeability and porosity; the variance of flow behavior index, initially low, increases in a linear fashion and almost reaches that of compressibility.

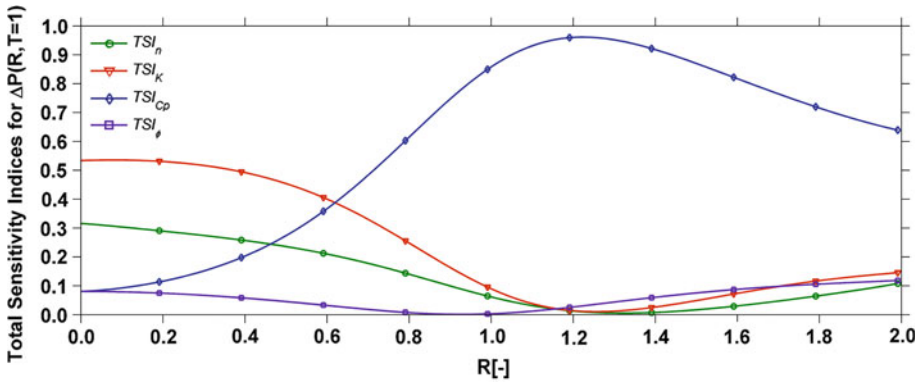


**Fig. 4** Total sensitivity indices ($TSI$) of each random parameter ($n, K, C_\mathrm{p}, \phi$) with respect to the excess pressure $\Delta P$ versus radial distance $R$ for cylindrical geometry ($d = 2$), $T = 1$, $S = 1$, and $r_\mathrm{c} = 1$

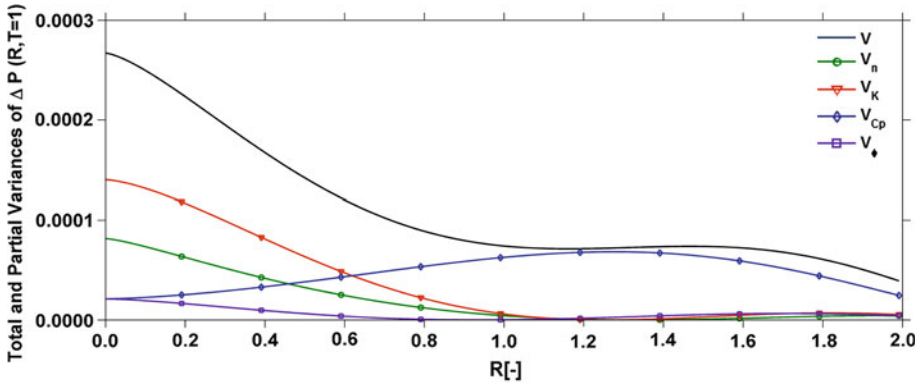


**Fig. 5** Total variance and partial variances ($V$) due to each random parameter ($n, K, C_\mathrm{p}, \phi$) with respect to the excess pressure $\Delta P$ versus radial distance $R$ for cylindrical geometry ($d = 2$), $T = 1$, $S = 1$, and $r_\mathrm{c} = 1$

Figure 4 shows the total sensitivity indices of each random parameter with respect to excess pressure as a function of space for fixed time $T = 1$. Figure 5 does the same for the variances. Close to the injection point, permeability and compressibility are the most influential variables, while the sensitivity to flow behavior index and porosity is low; as the distance from the injection point increases, compressibility becomes more important, until its sensitivity index is nearly one for $R \cong 1.25$. For $R > 1.25$, the importance of compressibility decreases in time, though it remains by far the most influential variable.

The total variance of the excess pressure decreases with increasing distance from the injection point, and approaches zero at the expected front position for $T = 1$. Close to the injection point, the larger contribution to the total variance is due to permeability and flow behavior index; the variance of compressibility increases linearly with distance and becomes dominant for $R > 1$; the porosity variance is low everywhere.

Results for a different value of time ($T = 0.1$) showed an overall trend of sensitivity indices and variances akin to that for $T = 1$.

An analogous analysis (not shown) conducted for plane ($d = 1$) and spherical ($d = 3$) geometry revealed that the behavior over time of sensitivity indices and variances of each

random parameter with respect to the front position was remarkably similar to that derived for the radial case, with minor differences linked to the higher values of the flow behavior index sensitivity index at very early and late times as the parameter $d$ increases from 1 to 3. When the sensitivity indices with respect to the excess pressure were considered as a function of $d$, the importance of compressibility, though remaining the highest, was seen to decrease as $d$ increases.

The results of the GSA via PCE have been compared with those deriving from a traditional Monte Carlo scheme to verify the accuracy of the proposed method.

## 6 Conclusions

In this article, we examined, with an analytical approach, the dynamics of pressure diffusion in unsteady non-Newtonian flows through porous media generated within the domain by an instantaneous mass injection in its origin. Via the adoption of a self-similar variable, we obtained a generalized closed-form solution, valid for plane, cylindrical, and semi-spherical geometry.

Expressing the model equations in dimensionless form, it was found that the variables of interest are functions of flow geometry, injected mass, fluid behavior index and dimensionless compressibility, and medium porosity.

For pseudoplastic fluids, we confirmed the existence of a pressure front traveling with finite velocity. Evaluation of the front position showed that the front advances farther in plane than in cylindrical or semi-spherical geometry; for a lower porosity, a larger flow behavior index, a lower compressibility, and a higher injected mass.

A GSA was conducted considering the fluid flow behavior index, and selected domain properties (permeability, porosity, and porous medium compressibility coefficient) as independent random variables having uniform distributions. The compressibility coefficient is the most influential variable affecting the evolution of the front position with time, followed by the flow behavior index.

The variation in space of the excess pressure at given time is most affected by the permeability near the injection point, while the influence of the compressibility prevails closer to the front position.

## A Appendix: Sensitivity Analysis Via Sobol' Indices

Because of the impossibility to characterize exhaustively the entire input parameter space of a given mathematical model, GSA is useful to evaluate the resulting effects on the uncertainty associated with model predictions. Moreover, the ability to identify the most influential input random variables with respect to the variance of the response allows to address investigations in order to improve the accuracy of model results (Saltelli et al. 2000).

### A.1 Sobol' Indices and ANOVA Representation

Among the possible choices of global sensitivity measures, the Sobol' indices have been widely used since they provide accurate information for a wide class of models (Sobol 1993; Archer et al. 1997). The ANOVA representation of a model, made by a finite set of terms

dependent on a growing number of uncertain variables (Archer et al. 1997), is useful for the definition of Sobol' indices.

Let $y = f(\mathbf{x})$ denote a scalar model function defined in $I^n$ (the $n$-dimensional unit hypercube), domain of the uncertain model parameters. If $f(\mathbf{x})$ is integrable over $I^n$, the following representation may be introduced:

$$f(\mathbf{x}) = f_0 + \sum_i f_i(x_i) + \sum_{i<j} f_{ij}(x_i, x_j) + \cdots f_{12\ldots n}(x_1, x_2, \ldots x_n), \tag{A.1}$$

$$\int_0^1 f_{i_1\ldots i_s}\left(x_{i_1}, \ldots x_{i_s}\right) dx_k = 0, \quad k = i_1, \ldots, i_s, \tag{A.2}$$

where $1 \le i_1 < \ldots < i_s \le n (s = 1, \ldots, n)$ are the indices specifying the parameters upon which each term depends and the $2^n$ summands in (A.1) are orthogonal functions that can be expressed as integrals of $f(\mathbf{x})$, e.g. $f_0 = \int f(\mathbf{x}) d\mathbf{x}$ is the mean of the model, $f_i(x_i) = \int f(\mathbf{x}) \Gamma_{k\neq i}\, d\mathbf{x}_k - f_0$ and so on. Therefore condition (A.2) renders representation (A.1), which is typically termed ANOVA decomposition, unique.

Now if $f(\mathbf{x})$ is square integrable, so are all the terms in (A.1). Then the total variance of the model, due to the uncertainty of its input parameters, is defined as:

$$V = \int_{I_n} f^2(\mathbf{x}) \cdot d\mathbf{x} - f_0^2. \tag{A.3}$$

Introducing the decomposition (A.1) into (A.3) allows to subdivide the total variance into the contributions $V_{i_1\ldots i_s}$, called partial variances:

$$V = \sum_{s=1}^{n} \sum_{i_1<\ldots<i_s}^{n} V_{i_1\ldots i_s}, \text{ with } V_{i_1\ldots i_s} = \int_{I_n} f_{i_1\ldots i_s}^2 \mathrm{d}x_{i_1} \ldots \mathrm{d}x_{i_s} \tag{A.4}$$

Now the generic $s$-order Sobol' index $S_{i_1\ldots i_s}$ is defined by the ratio (Sobol 1993):

$$S_{i_1\ldots i_s} = V_{i_1\ldots i_s} / V, \tag{A.5}$$

it is immediate to verify that the sum of all indices up to $n$-order is equal to one. Among these, the first order indices $S_i$, or principal sensitivity indices, describe the share of total variance due to the uncertainty of each parameter, when individually considered. The total sensitivity indices, on the other hand, evaluate the overall effect of a parameter, when all its possible interactions with other parameters are considered:

$$S_{T_i} = \sum_{\eta_i} S_{i_1,\ldots i_s}, \quad \eta_i = \{(i_1, \ldots i_s) : \exists k, 1 \le k \le s, i_k = i\}. \tag{A.6}$$

A complete GSA requires the estimation of $2^n$ integrals; this is generally done by Monte Carlo simulations (Sobol 2001); the computational cost associated with this procedure is prohibitive when the model is complex and the number of uncertain parameters is large (Sudret 2008).

### A. 2 PCE method

The PCE theory, developed in the 30s (Wiener 1938), may be considered a viable and convenient method for Sobol' indices estimation.

Let $S$ denote a stochastic model with a finite number $M$ of input random variables. The PCE $\tilde{S}$ of $S$ is defined by a polynomial basis in the Hilbert space containing the response:

$$S(X_1, \ldots X_M) \cong \tilde{S}(\zeta_1, \ldots \zeta_M) = \sum_{j=0}^{P-1} s_j \Psi_j(\zeta_1, \ldots \zeta_M) \text{ with } P = \frac{(M+p)!}{M!p!}, \quad \text{(A.7)}$$

where $\Psi_j$ denotes the $j$-order multivariate orthogonal polynomial, and $\{\zeta_i\}_{i=1}^{M}$ is the set of independent random variables, whose probability distribution function is linked to the choice of the polynomial basis (Xiu and Karniadakis 2002); $s_j$ are the polynomial coefficients.

Note that the applicability of the method is independent from the distribution of the input random variables of the model $S$ gathered in $\mathbf{X}$. In fact, if such distribution doesn't match the required distribution for the use of the chosen polynomial basis, is sufficient to apply an isoprobabilistic transform to tie $\mathbf{X}$ and $\zeta$.

To settle the PC expansion, it is necessary to define the coefficients $s_j$; one possibility consists in a regression method based on the minimization of the variance of a residual $\varepsilon$ defined as the difference between the surrogate model response, $\tilde{S}$, and the exact solution given by the original model (Sudret 2008):

$$\varepsilon = S(\mathbf{X}) - \tilde{S}(\boldsymbol{\zeta}) = S(\mathbf{X}) - \sum_{j=0}^{P-1} s_j \Psi_j(\boldsymbol{\zeta}). \quad \text{(A.8)}$$

The vector of the unknown coefficients $\boldsymbol{\varsigma}$ results then:

$$\boldsymbol{\varsigma} = \text{Min}\left\{ E\left[ \left( S(\mathbf{X}(\boldsymbol{\zeta})) - \tilde{S}(\boldsymbol{\zeta}) \right)^2 \right] \right\}. \quad \text{(A.9)}$$

where $E[\cdot]$ denotes the expected value.

Is useful to rewrite (A.9) as:

$$\boldsymbol{\varsigma} = \left( \boldsymbol{\Psi}^T \boldsymbol{\Psi} \right)^{-1} \cdot \boldsymbol{\Psi}^T \cdot S', \boldsymbol{\Psi}_{ij} = \Psi_j\left(\zeta^i\right); i = 1, \ldots N; j = 0, \ldots P-1, \quad \text{(A.10)}$$

where $N$ is the number of regression points, $S'$ is the vector denoting the model response at these $N$ points, while the product $\boldsymbol{\Psi}^T \boldsymbol{\Psi}$ defines the so-called information matrix.

The optimal set of regression points is constituted by the integration points of the Gaussian quadrature (Huang et al. 2007). Solution of (A.10) requires a minimum number of points equal to $P$. On the other hand, since the points choice is conditioned, generally one has $N > P$; in this case the information matrix is not singular.

Note that the entire variability of the original model is conserved, being embedded in the set of PCE coefficients. Hence, once the coefficients are available, the Sobol' indices can be analytically defined without further computational costs.

Gathering, as in (A.1), the terms in the expansion according to the variables they depend on, it is easy to isolate the different influences on the response (Sudret 2008):

$$\begin{aligned} \tilde{S}(\boldsymbol{\zeta}) = s_0 &+ \sum_{i=1}^{n} \sum_{\alpha \in \varphi_i} s_\alpha \Psi_\alpha(\zeta_i) \\ &+ \sum_{1 \le i_1 < \ldots < i_s \le n}^{n} \sum_{\alpha \in \varphi_{i_1, \ldots, i_s}} s_\alpha \Psi_\alpha(\zeta_{i_1}, \ldots, \zeta_{i_s}) + \ldots \\ &+ \sum_{\alpha \in \varphi_{1,2 \ldots n}} s_\alpha \Psi_\alpha(\zeta_1, \ldots, \zeta_n) \end{aligned} \quad \text{(A.11)}$$

where $\varphi$ explains in subscript the set of input parameters each multidimensional polynomial really depends on.

In this sense, the PC expansion is similar to the ANOVA representation of the model, but computationally more advantageous. In fact, given the orthogonality of the polynomial basis, it is immediate to observe that the mean of the response coincides with the coefficient associated to the zero-grade term, while the total variance, calculated with the surrogate model, is:

$$V_{\tilde{S}} = \mathrm{Var}\left[\sum_{j=0}^{P-1} s_j \Psi_j(\boldsymbol{\zeta})\right] = \sum_{j=1}^{P-1} s_j^2 E\left[\Psi_j^2(\boldsymbol{\zeta})\right]. \tag{A.12}$$

Finally, the Sobol' indices can be derived as:

$$S_{i_1,\ldots i_s} = \frac{\sum_{\alpha\in\varphi_{i_1,\ldots,i_s}} s_\alpha^2 E\left[\Psi_\alpha^2\right]}{V_{\tilde{S}}}. \tag{A.13}$$

The expected value of the squares of polynomials appearing in (A.13) may be evaluated as illustrated in Abramowitz and Stegun (1970).

## References


Abramowitz, M., Stegun, I.A.: Handbook of Mathematical Functions. Dover Publications, New York (1970)

Archer, G.E.B., Saltelli, A., Sobol, I.M.: Sensitivity measures, ANOVA like techniques and the use of bootstrap. J. Stat. Comput. Simul. **58**, 99–120 (1997)

Barenblatt, G.I.: Scaling, Self-Similarity, and Intermediate Asymptotics. Cambridge University Press, Cambridge (1996)

Bird, R.B., Stewart, W.E., Lightfoot, E.N.: Transport Phenomena. Wiley, New York (1960)

Chhabra, R.P., Comiti, J., Machač, I.: Flow of non-Newtonian fluids in fixed and fluidised beds. Chem. Eng. Sci. **56**, 1–27 (2001)

Christopher, R.H., Middleman, S.: Power-law flow through a packed tube. I&EC Fundam. **4**(4), 422–426 (1965)

Di Federico, V., Pinelli, M., Ugarelli, R.: Estimates of effective permeability for non-Newtonian fluid flow in randomly heterogeneous porous media. Stoch. Environ. Res. Risk Assess. **24**, 55–69 (2010)

Di Federico, V., Ciriello, V.: Non-Newtonian flow through porous media due to an instantaneous mass injection. In: Proceedings AIMETA 2011, Italian Association of Theoretical and Applied Mechanics, Bologna, 12–15 September 2011, pp. 1–9 (2011)

Ghanem, R.G., Spanos, P.D.: Stochastic finite elements—a spectral approach. Springer, Berlin (1991)

Goldstein, R.V., Entov, V.M.: Quantitative Methods in Continuum Mechanics. Wiley, New York (1994)

Gradshteyn, I.S, Ryzhik, I.M.: Table of Integrals, Series and Products. Academic Press, San Diego (2000)

Huang, S., Sankaran, M., Ramesh, R.: Collocation-based stochastic finite element analysis for random field problems. Probab. Eng. Mech. **22**, 194–205 (2007)

Kozicki, W., Hsu, C.J., Tiu, C.: Non-Newtonian flow through packed beds and porous media. Chem. Eng. Sci. **22**, 487–502 (1967)

Ostendorf, W., DeGroot, D.J., Judge, A.I., LaMesa, D.F.: Method to characterize aquitards above leaky aquifers with water supply wells. Hydrogeol. J. **18**, 595–605 (2010)

Park, H.C., Hawley, M.C., Blanks, R.F.: The flow of non-Newtonian solutions through packed beds. Polym. Eng. Sci. **15**(11), 761–773 (1975)

Pascal, H.: On non-linear effects in unsteady flows through porous media. Int. J. Nonlinear Mech. **26**(2), 251–261 (1991a)

Pascal, H.: On propagation of pressure disturbances in a non-Newtonian fluid flowing through a porous medium. Int. J. Nonlinear Mech. **26**(5), 475–485 (1991b)

Pascal, H., Pascal, F.: Flow of non-Newtonian fluid through porous media. Int. J. Eng. Sci. **23**(5), 571–585 (1985)

Pascal, J.P., Pascal, H.: Nonlinear effects on some unsteady non-Darcian flows through porous media. Int. J. Nonlinear Mech. **32**(2), 361–376 (1997)

Pearson, J.R.A., Tardy, P.M.J.: Models of non-Newtonian and complex fluids through porous media. J. Non-Newton Fluid Mech. **102**(2), 447–473 (2002)

Saltelli, A., Chan, K., Scott, EM.: Sensitivity Analysis. Wiley, New York (2000)
Savins, J.G.: Non-Newtonian flow through porous media. Ind. Eng. Chem. **6**(10), 18–47 (1969)
Shenoy, A.V.: Non-Newtonian fluid heat transfer in porous media. Adv. Heat Transf. **24**, 102–190 (1995)
Sobol, I.M.: Sensitivity estimates for nonlinear mathematical models. Math. Model. Comput. **1**, 407–414 (1993)
Sobol, I.M.: Global sensitivity indices for nonlinear mathematical models and their Monte Carlo estimates. Math. Comput. Simul. **55**, 271–280 (2001)
Sochi, T.: Flow of Non-Newtonian fluids in porous media. J. Polym. Sci. B **48**, 2437–2767 (2010)
Sudret, B.: Global sensitivity analysis using polynomial chaos expansions. Reliab. Eng. Syst. Saf. **93**, 964–979 (2008)
Teeuw, D., Hesselink, F.T.: Power-law flow and hydrodynamic behavior of biopolymer solutions in porous media. In: Proceedings of Fifth International Symposium on Oilfield and Geothermal Chemistry, SPE Paper 8982, pp. 73–86 (1980)
Thibeau, S., Mucha, V.: Have we overestimated saline aquifer $CO_2$ storage capacities?. Oil Gas Sci. Technol. Rev. IFP Energ. Nouv. **66**(1), 81–92 (2011)
Wiener, N.: The homogeneous chaos. Am. J. Math. **60**, 897–936 (1938)
Wu, Y.S., Pruess, K.: A numerical method for simulating non-Newtonian fluid flow and displacement in porous media. Adv. Water Res. **21**, 351–362 (1998)
Xiu, D., Karniadakis, G.E.: The Wiener-Askey polynomial chaos for stochastic differential equations. J. Sci. Comput. **24**(2), 619–644 (2002)